Heliyon 9 (2023) e18471

Contents lists available at ScienceDirect

Heliyon

journal homepage: www.cell.com/heliyon

Quantitative analysis of a posterior fossa teratomas with unusual CT and MR Characteristics——illustrative case

Ying Huang [a,b,d], Yu Dong [a], Ping Li [a], Chuan Zhou [a], Wei-Xin Li [a], Zai-Jun Li [e], Yi Liu [f], Yu-Hai Bao [a,c,d,**], Duan-Fang Liao [b,*]

[a] Department of Neurosurgery, Shenzhen Samii Medical Center, Shenzhen, Guangdong, China
[b] Key Laboratory for Quality Evaluation of Bulk Herbs of Hunan Province, Hunan University of Chinese Medicine, Changsha, China
[c] Department of Neurosurgery, Xuanwu Hospital Capital Medical University, Beijing, China
[d] China International Neuroscience Institute, Beijing, China
[e] Medical Imaging Department, Shenzhen Samii Medical Center, Shenzhen, Guangdong, China
[f] Clinical Laboratory, Shenzhen Samii Medical Center, Shenzhen, Guangdong, China

ARTICLE INFO

Keywords:
Teratoma
Intracranial cysts
Magnetic resonance imaging
Magnetic resonance tissue characterization

ABSTRACT

Background: Intracranial teratomas or other cystic lesions with atypical imaging manifestations can still be frequently seen clinically. The specific reasons for unusual imaging manifestations need to be further explored.

Observation(s): A case of adult teratoma in the posterior fossa with unusual imaging manifestations was reported. The chemical composition of its cystic fluid was quantitatively detected, and in vitro imaging simulation experiments were performed on some fluid substances with similar cystic fluid properties to explore the reasons for special imaging manifestations. The content of inorganic substances and protein in the cystic fluid were both low, with no melanin detected. In vitro experiments revealed that MR T1 signals could increase with protein content rising and changes in MR T2 signals presented no obvious correlation with it. CT values increased gradually with protein concentration rising. The substances with similar viscosity had similar CT values, whereas substance viscosity showed no significant correlation with changes in MR signals.

Conclusion: The abnormality of imaging manifestations cannot be confirmed as the result of "high protein content", nor can it be simply attributed to bleeding. Further research is required for the impact of the combination of paramagnetic particles and biofluid on imaging.

1. Introduction

Teratoma, a term originating from the Greek word "teras," meaning "monster," has been the subject of understanding and research in the medical field since Johannes Scultetus first reported a case of mature cystic teratoma in 1659 [1]. While past studies have provided us with a foundation of knowledge about teratomas, there remain uncertainties and challenges in its radiological manifestations.

* Corresponding author. Key Laboratory for Quality Evaluation of Bulk Herbs of Hunan Province, Hunan University of Chinese Medicine, Xueshi Rd, NO. 300, Hanpu Science & Education District, Changsha, 410208, Hunan, China.

** Corresponding author. Department of Neurosurgery, Xuanwu Hospital Capital Medical University, Changchun St, NO.45, Xicheng District, Beijing 100053, China.

E-mail addresses: baoyuhai@126.com (Y.-H. Bao), dfliao@hnucm.edu.cn (D.-F. Liao).

https://doi.org/10.1016/j.heliyon.2023.e18471
Received 28 March 2023; Received in revised form 16 July 2023; Accepted 18 July 2023
Available online 20 July 2023

Teratomas consist of tissues from multiple germ layers, and the heterogeneity of these tissues largely contributes to the diversity of its radiological manifestations [2]. Solid teratomas, with their various admixed tissues and cellular components such as fat and calcium, often present distinctive radiological characteristics which aid in differential diagnosis [3,4]. However, the radiological manifestations of cystic teratomas often resemble other intracranial cystic lesions, such as epidermoid cysts, dermoid cysts, colloid cysts, and arachnoid cysts, even intracranial hematoma, making the differential diagnosis challenging [5–7].

In light of this, we report a peculiar case of posterior fossa teratoma in an adult. The radiological manifestation of this case defies traditional understanding. The lesion primarily appears cystic with CT revealing slightly hyperdense, and MRI showing high signal on T1 and low signal on T2. These characteristics led to a preoperative misdiagnosis of the lesion as either an epidermoid or a colloid cyst. In response to this unusual radiological presentation, we have analyzed its histological components and conducted in vitro simulation experiments. Combined with existing literature, we have made preliminary explorations into its possible imaging causes.

The aim of our research is to enhance our understanding of the radiological manifestations of cystic lesions through this peculiar case of posterior fossa teratoma and to propose new possible diagnostic and differential diagnostic approaches.

1.1. Illustrative cases

Case reports: A 36-year-old female began to have intermittent dizziness and blurred vision without obvious inducement 18 years ago, accompanied with nausea and vomiting. The symptoms improved after vomiting, and no examination and treatment was given. In May 2020, the patient began to suffer from posterior occipital tingling, which was aggravated when the emotion was agitated. After a few minutes, it could subside spontaneously. The symptoms such as dizziness and vomiting appeared more frequently than before. In September 2021, the patient visited the outpatient department in our hospital. The head CT results showed as follows: irregular high-density mass shadow in the posterior fossa; the CT value of about 93HU; few bone density shadows seen at the posterior edge (Fig. 1A).

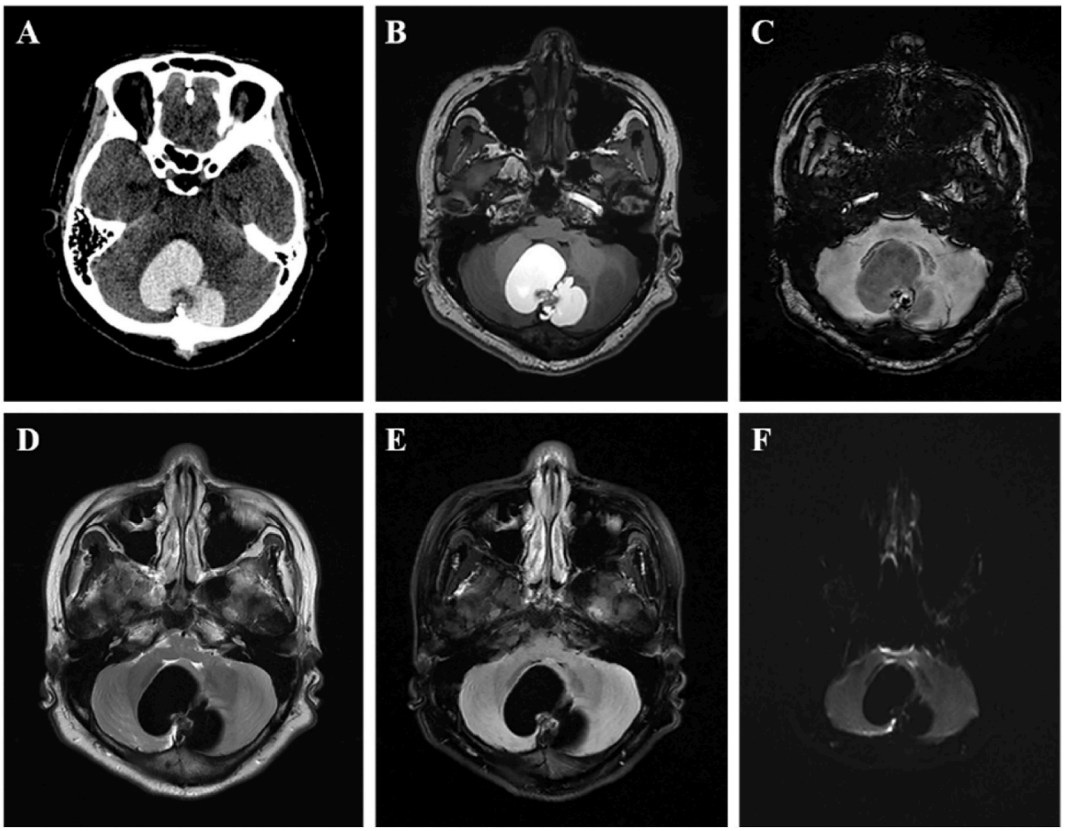

Fig. 1. Axial CT showed as follows: Irregular high-density mass shadows in the posterior fossa, with a CT value of about 93HU; few bones density shadows visible at the posterior edge, with the compression of adjacent bilateral cerebellar hemispheres and brainstem, and narrowing of the fourth ventricle (A). MR imaging showed irregular mixed signals distributed across the midline in the medial and posterior cerebellum, with a maximum diameter of about 50 mm × 41 mm × 51 mm. Line-like septum and complex nodules with a slightly irregular shape were visible inside the cyst, with the nodule size of about 15 mm × 16 mm × 13 mm (maximum oblique diameter). The brain parenchyma around the lesion was compressed, with slight narrowing of the fourth ventricle. T1WI (B) of the cystic part was mainly equal or high signals. T2WI (D) and T2 flair (E) both showed low signals. DWI sequence (F) showed low signals, with no diffusion restriction in mural nodules and septum; multiple patchy low signals and high signals were visible in the nodular of SWI sequence (C).

MR showed cystic space-occupying in the posterior fossa, with the consideration of the possibility of atypical dermoid cysts or atypical colloid cysts (containing calcification and blood vessel protein components, as well as bleeding and colloid ones) were considered (Fig. 1B, C, 1D, 1E, 1F).

The patient consented to the procedure and underwent surgery in October 2021. The suboccipital posterior median approach was adopted and the arachnoid-encapsulated cyst visible at the median position of the cerebellum. After the arachnoid was cut open, the dark green turbid and highly viscous colloid cyst fluid was seen flowing out. The small nodule part located in the median cerebellum was generally faint yellow, with tooth-like calcification, white hair and fat-like components visible inside it (Fig. 2A and B). The patient had no the symptoms such as dizziness, headache, vomiting and neurological dysfunction after surgery. The cerebrospinal fluid examination showed AFP (−) and β- HCG (−). The patient reported feeling good after discharge.

Upon pathological evaluation, the internal constituents of the cystic component were observed to be an amalgamation of sheet-like particulate matter, stained in a powdery pattern, with non-structural matter, and crystalline formations of cholesterol. Notably, no indications of hemorrhagic foci were observed. Examination of the tumorous nodules revealed the presence of stratified squamous epithelium, sweat glands, and hair follicle-like skin appendages, with an interspersed stroma consisting of proliferative fibrous connective tissue. These pathological features coalesce to confirm the diagnosis of a mature cystic teratoma. (Fig. 2C and D). Analysis of proteolipids and inorganic components in cyst fluid in patients with teratoma was carried out, with the quantitative detection of the melanin content by ELISA. The results showed that the contents of total protein, albumin, globulin, total cholesterol and triglyceride inside the cyst fluid were 15 g/l, 6.4 g/l, 8.6 g/l, 0.71 mmol/l and 0.3 mmol/l, respectively. The highest inorganic content was sodium (1667 mg/kg), followed by potassium (317 mg/kg), calcium (300 mg/kg), magnesium (104 mg/kg), iron (64 mg/kg) and copper (5.6 mg/kg), respectively (Table 1). Melanin was not detected.

In vitro simulation experiments: Due to the complexity of various biological fluids in the body, the viscous cyst fluid may not consist of only protein polymers, but carbohydrates such as hyaluronic acid. In order to further confirm whether there is a correlation of protein concentration and substance viscosity with MR and CT signals, and whether other biological fluid substances may cause signal changes, some in vitro imaging simulation experiments of fluid substances similar to cyst fluid properties were conducted by us (Supplement Table 1). The detection results are shown in Fig. 3A–C.

For albumin solutions with concentrations ranging from 15 g/l to 175 g/l, CT signals appeared to increase with the concentration of protein but the changes were not pronounced (A). Materials with similar viscosity exhibited similar CT values (A). Rising protein concentration heightened MR T1 signal intensity (B), but showed no clear correlation with MR T2 signal (C). No evident correlation was observed between material viscosity characteristics and changes in MR T1 and T2 signals (B, C). Interestingly, collagen solution displayed high signals on both CT and MR T1 and T2 imaging (A, B, C), which can be explained by its relatively lower viscosity and higher free water content from the high-purity collagen powder dissolved in saline for preparation. The reasons for its high signal on both CT and MR T1 remain unclear.

2. Discussion

Intracranial mature teratomas are complex tumors with diverse imaging characteristics that can be challenging to distinguish from

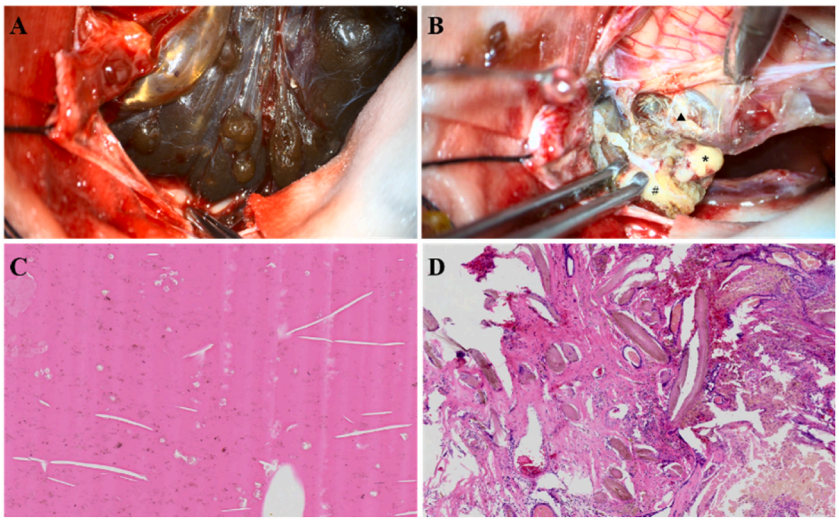

Fig. 2. During surgery, the following could be seen: (A) The cyst was encapsulated by the thin arachnoid membrane, and its contents were dark green viscous jelly-like; (B) The diseased nodular part was faint yellow, with hair (▲), tooth-like calcifications (#) and fat like substances visible (*). Under the light microscope, (C) the substance in the cyst was flaky powder dyed, unstructured substance and cholesterol crystals, with no sign of bleeding; (D) stratified squamous epithelium, sweat glands and hair follicle skin appendages were visible in the partial tissue of the nodule and the interstitium was hyperplastic fibrous connective tissue.

Table 1
Contents of protein, lipid and inorganic substances in cyst fluid.

Items	Results	Items	Results (mg/kg)
Total protein (TP)	15 g/l	Sodium (Na)	1667
Albumin (ALB)	6.4 g/l	Kalium (K)	317
Globulin (GBL)	8.6 g/l	Calcium (Ca)	300
Prealbumin (PAB)	0.02 g/l	Magnesium (Mg)	104
Total bile acid (TBA)	0.1 μmol/l	Iron (Fe)	64
Total cholesterol (TC)	0.71 mmol/l	Copper (Cu)	5.6
Triglyceride (TG)	0.3 mmol/l	Aluminium (Al)	2.2
HDL-C	0.01 mmol/l	Zinc (Zn)	2.1
LDL-C	0.09 mmol/l	Strontium (Sr)	0.33
Lipoprotein a (LP-a)	0.3 nmol/l	Rubidium (Rb)	0.24

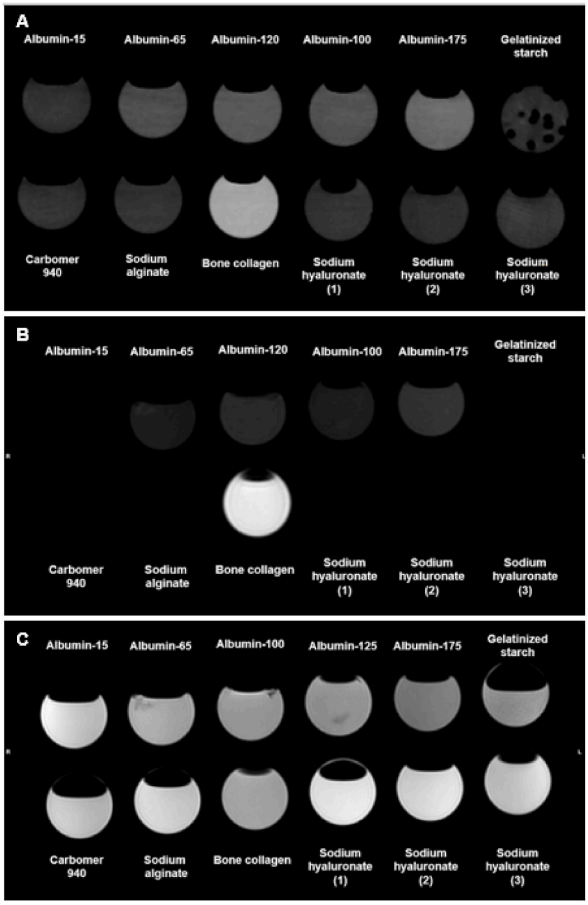

Fig. 3. The Imaging examination results of different fluids. (GE 64 row 128 slice CT (Optima680) and 3.0T MR (Philips Ingenia) imaging systems were adopted for scanning.) CT and MR imaging results of different fluid substances are illustrated (refer to labels and Supplement Table 1 for fluid names and compositions). (A) CT; (B) MR T1WI; (C) MR T2WI.

other intracranial cystic lesions, including epidermoid cysts, dermoid cysts, arachnoid cysts, and colloid cysts, particularly when presenting with atypical imaging features such as "white epidermoid cysts" [5–7]. In our case, the patient's CT scan showed slightly high density, MR T1 showed slightly high signal, and T2 showed low signal, leading to a preoperative suspicion of an epidermoid or colloid cyst. However, postoperative pathology revealed a teratoma. Previous literature reports only one case of posterior fossa mature teratoma, two cases of posterior fossa epidermoid cyst, and two cases of anterior fossa epidermoid cyst with similar imaging features [8–11]. The specific reasons for these atypical imaging features require further investigation.

Formerly, intracranial cystic lesions such as epidermoid cysts, dermoid cysts, and teratomas were thought to exhibit high-density signals on CT imaging primarily due to the high protein concentration of the cystic fluid, after excluding factors such as hemorrhage or calcification [12–15]. Lipper et al. and Timmer et al. reported cystic fluid protein concentrations as high as 173 g/l and 210 g/l

Table 2
Cyst fluid components and imaging manifestations.

NO.	CT	T1	T2	Total protein (TP) (g/l)	Cholesterol (Chol)	Triglyceride (TG)	Others	General
Ochi et al., 1998 [22]	H	H	H	291	–	32mg/dl (0.36mmol/l)	–	greenish semi-liquid material containing debris
Timmer et al., 1998 [17]	H	slightly H	H	210	336mg/dl (8.7 mmol/l)	417mg/dl (4.7 mmol/l)	albumin 140 g/l, calcium 150 mg/kg, iron 26 mg/kg, copper 3 mg/kg, nickel 0.5 mg/kg, and manganese 0.2 mg/kg	a dark brown cyst with highly viscous, toffee-like contents
Kuwabara et al., 1987 [23]	slightly H	–	–	200	–	–	calcium 10.6 mg/dl, iron 5.8 mg/dl, magnesium 4.1 mg/dl, copper 0.3 mg/dl	turbid dark brown fluid (glittering cholesterol crystals)
Lipper et al., 1981 [16]	H	–	–	173	413mg/dl (10.69mmol/l)	–	–	–
Braun et al., 1982 [15]	slightly H	–	–	152	–	–	–	"Crankcase oil"
Daugherty et al., 2016 [8]	H or Iso-	H	H	124	187mg/dl (4.84mmol/l)	65mg/dl (0.73mmol/l)	–	semiviscous
Ahmadi et al.,1994 [24]	H or Iso-	H	H	112	1894mg/dl (49mmol/l)	808mg/dl (9.09mmol/l)	–	semiviscous
Ahmadi et al.,1994 [24]	H or Iso-	H	H	104	144mg/dl (3.72mmol/l)	8mg/dl (0.09mmol/l)	hemoglobin 40g/l (methemoglobin 18%)	semiviscous
Nagasawa et al.,1983 [25]	Iso-	–	–	92	–	–	–	dark brown fluid with cholesterin crystals
Ahmadi et al., 1992 [26]	–	Iso-	–	90	90mg/dl (2.33mmol/l)	22mg/dl (0.25mmol/l)	–	–
Ahmadi et al., 1992 [26]	–	H	–	86	168mg/dl (4.34mmol/l)	54mg/dl (0.61mmol/l)	hemoglobin 30g/l (methemoglobin 14%)	–
Ahmadi et al., 1992 [26]	–	H	–	83	176mg/dl (4.55mmol/l)	66mg/dl (0.74mmol/l)	hemoglobin 30g/l (methemoglobin 15%)	–
Hackney et al., 1987 [27]	–	L	–	65	270mg/dl (6.98mmol/l)	63mg/dl (0.71mmol/l)	–	–
Braun et al., 1982 [15]	H	–	–	55	–	–	calcium 8.6 mg/dl, iron 180 μg/dl	–
Hackney et al., 1987 [27]	–	L	–	54	149mg/dl (3.85mmol/l)	50mg/dl (0.56mmol/l)	–	–
Hackney et al., 1987 [27]	–	L	–	49	185mg/dl (4.78mmol/l)	62mg/dl (0.70mmol/l)	–	–
Hackney et al., 1987 [27]	–	L	–	43	228mg/dl (5.9mmol/l)	84mg/dl (0.95mmol/l)	–	–
Hackney et al., 1987 [27]	–	L	–	41	135mg/dl (3.49mmol/l)	42mg/dl (0.47mmol/l)	–	–
Braun et al., 1982 [15]	H	–	–	38	–	–	calcium 8.6 mg/dl, iron 246 μg/dl	xanthochromic fluid
Gupta et al.,1993 [28]	–	L	L	–	–	–	iron 19.63, copper 2.99, magnesium 41.11 μg/g	–
Gupta et al.,1993 [28]	–	H	L	–	–	–	iron 18.24, copper 2.80, magnesium 42.21 μg/g	–
Gupta et al.,1993 [28]	–	Iso-	Iso-	–	–	–	iron 202, copper 35, magnesium 648 μg/g	–
Isiklar et al., 1995 [29]	–	H	L	–	–	–	more than 10% melanotic cells	–
Kim et al., 2000 [30]	–	H	L	–	–	–	Melanin ++	solid

H, high/hyperintensity; L, low/hypointensity; Iso-, isodense/isointensity.

(albumin 140 g/l), displaying a high-density signal on CT imaging [16,17]. However, after reviewing the literature on cystic fluid components and imaging features (Table 2), it was discovered that a CT high-density signal could occur when the cystic fluid protein concentration was as low as 38 g/l or 55 g/l, and the proportion of protein content did not demonstrate a significant correlation with imaging features [18–21]. In our case, the total protein content of the cystic fluid was only 15 g/l (albumin 6.4 g/l), yet it still presented a high-density signal. Consequently, we conducted in vitro simulation experiments using albumin concentrations ranging from 15 g/l to 175 g/l for CT scanning, which revealed that although the CT signal intensity appeared to increase with increasing protein concentration, the change was insignificant (Fig. 3A). Therefore, it is believed that the high-density signal on CT cannot solely be attributed to the "high protein content" of the cystic fluid after excluding hemorrhage or calcification.

The composition of intracranial cystic lesions, including epidermoid cysts, dermoid cysts, and teratomas, consists of epithelial debris, keratin, mucin, cholesterol, and unsaturated fatty acids. Early hypotheses suggested that the high signal intensity of these lesions on MR T1-weighted imaging was due to a combination of protein, hemorrhage, cholesterol, and other fatty substances [31,32]. However, subsequent studies showed that cholesterol and triglycerides were not responsible for the T1 high signal intensity, and the low-density lipoprotein signal intensity change was minimal and difficult to detect at concentrations of 0–61g/l [26,27]. On 1.5T MR imaging, there is no significant T1 change when the albumin concentration is less than 80g/l [33]. However, higher concentrations of proteins ($\geq$90g/l) and free hemoglobin can increase the T1 signal intensity of cyst fluid [26].

On MR T2-weighted imaging, the signal intensity of intracranial cystic lesions, including teratomas, can decrease with increasing protein concentration due to extensive cross-linking between proteins, as well as with increasing viscosity, which mainly reflects water content [19]. Therefore, high signal intensity on both T1 and T2 images is believed to be caused by the semi-liquid cystic contents with high protein concentrations [34,22]. In some cases, the high signal intensity on T1-weighted images may be due to the paramagnetic effect of ferric ion (Fe3+) from intracystic hemorrhage [16,35,36]. If the T1 signal is high and the T2 signal is low, it may be due to more viscous "taffy-like content," which combines the characteristics of high protein content and high viscosity, similar to chronic nasal secretions, or due to the deposition of intracystic hemosiderin, which appears as a brown oily substance [17,37].

Therefore, high viscosity is also a feature often associated with imaging characteristics of these cystic lesions. In our case, although the cyst fluid protein concentration was only 15g/l, the cyst fluid had high viscosity. Thus, in our simulation experiment (3.0T MR), we selected substances with similar viscosity to the cyst fluid for imaging, in addition to selecting gradient concentration protein solutions. The results showed that increasing protein concentration enhanced MR T1 signal intensity, but substance viscosity did not show a clear correlation with MR signal changes (Fig. 3B–C), and substances with similar viscosity had similar CT values. Therefore, it is not appropriate to solely attribute anomalous CT and MR imaging features of intracranial cystic lesions to "high protein concentration" or "high viscosity."

The inorganic components, notably metal ions, within the lesion's cystic fluid have significant implications for imaging manifestations. Our cystic fluid's analysis revealed that sodium (1667 mg/kg or 72.5 mmol/kg) was the most abundant inorganic substance, with concentrations exceeding average sodium ion concentration in brain tissue (48 $\pm$ 1 mmol/l in gray matter, 43 $\pm$ 3 mmol/kg in white matter) but lower than that in cerebrospinal fluid (129 $\pm$ 8 mmol/l in sulci, 138 $\pm$ 4 mmol/kg in ventricles) [38]. The contents of iron, manganese, and other elements were comparatively lower.

Though literature lacks a direct correlation between trace inorganic elements and imaging manifestations, it is crucial to explore their potential impact. The effects of paramagnetic ions, such as sodium, potassium, iron, and manganese, may be more significant on MR examination results than anticipated, possibly contributing to our case's unusual imaging manifestations [39–42]. Nevertheless, paramagnetic ions' effect in pure water doesn't necessarily reflect their behavior when bound to macromolecules, suggesting even at relatively low concentrations, they may significantly affect relaxation times.

Considering the inherent complexity of biological fluids in vivo, it's challenging to extrapolate the impacts of metal ions or other substances on proton relaxation from in vitro studies. Therefore, a thorough analysis of the paramagnetic compounds and molecular composition of fluids might be necessary for understanding the diverse signal characteristics of the cystic fluid, which cannot be explained by a single factor.

In addition to the inorganic constituents, the possibility of melanin, given its paramagnetism, is worth exploring. Though no melanin was detected in our analysis, lesions containing even over 10% melanin may exhibit high T1 signal and low T2 signal [29,30,43]. However, determining the melanin content that can significantly affect MR signal changes warrants further investigation. The presence of other biotin-like paramagnetic substances, which could accumulate under pathological conditions, also remains an open question.

3. Conclusion

In summary, when encountering intracranial cystic lesions with atypical imaging features, it is inadequate to attribute them solely to factors such as "high protein content", "high viscosity", or "bleeding". The presence of inorganic or organic substances beyond physiological ranges in pathological conditions and their interactions with proteins and other substances in different ways can lead to signal changes. Moreover, the potential impact of biomolecules containing paramagnetic substances, such as melanin, on imaging findings should also be taken into account. Further investigations are required to better understand the effects of the combination of paramagnetic particles and biological fluids on imaging.

4. Limitations

While we have endeavored to shed light on the unusual imaging manifestations, this study does have certain limitations. Firstly, we

were unable to identify all constituents of the cystic fluid, preventing a definitive explanation for the atypical imaging outcomes. Rather, we proposed potential hypotheses based on existing literature and our experimental results, offering a foundation for future investigations. Our findings, rooted in a single case study, may also limit the generalizability of our conclusions, emphasizing the necessity of larger, more comprehensive studies. In addition, our simulation model did not accurately mimic the exact viscosity of the cystic fluid and relied on literature-derived parameters for gradient protein solutions, possibly hindering the precise replication of in vivo conditions. Consequently, future research is required to delve deeper into the impact of proteins, inorganic ions, and melanin on imaging presentations to fully grasp the intricate interplay among these components. While these limitations exist, we believe that our study provides a crucial step towards understanding this complex field.

Author contribution statement

All authors listed have significantly contributed to the investigation, development and writing of this article.

Data availability statement

No data was used for the research described in the article.

Funding

This study was jointly funded by the Shenzhen Samii Medical Center (Project No. SSMC-2021-A9) and the Natural Science Foundation of Hunan Province (Project No. 2022JJ30454).

Declaration of competing interest

The authors declare that they have no known competing financial interests or personal relationships that could have appeared to influence the work reported in this paper.

Acknowledgement

The authors would like to thank Ms. Juan Tang (Shenzhen GD, China) for her kind technical assistance.

Appendix A. Supplementary data

Supplementary data to this article can be found online at https://doi.org/10.1016/j.heliyon.2023.e18471.

References

[1] A. Ahmed, S. Lotfollahzadeh, Cystic teratoma. 2022 dec 3, in: StatPearls, StatPearls Publishing, Treasure Island (FL), 2023. Jan–. PMID: 33231995.
[2] WHO Classification of Tumours Editorial Board, World Health Organization Classification of Tumours of the Central Nervous System, fifth ed., International Agency for Research on Cancer, Lyon, 2021.
[3] A.G. Osborn, M.T. Preece, Intracranial cysts: radiologic-pathologic correlation and imaging approach, Radiology 239 (3) (2006) 650, https://doi.org/10.1148/radiol.2393050823.
[4] E. Arslan, H. Usul, S. Baykal, E. Acar, E.E. Eyüboğlu, A. Reis, Massive congenital intracranial immature teratoma of the lateral ventricle with retro-orbital extension: a case report and review of the literature, Pediatr. Neurosurg. 43 (4) (2007) 338–342, https://doi.org/10.1159/000103319.
[5] J. Gosal, J. Joseph, D. Khatri, K.K. Das, A. Jaiswal, A. Gupta, White epidermoid of the sylvian fissure masquerading as a dermoid cyst: an extremely rare occurrence, Asian J Neurosurg 14 (2) (2019) 553–556, https://doi.org/10.4103/ajns.AJNS_241_18.
[6] J.S. Gosal, M. Garg, S. Tiwari, K.K. Das, D.K. Jha, White epidermoid: an important radiological mimic of the dermoid, Childs Nerv Syst 37 (3) (2021) 737–738, https://doi.org/10.1007/s00381-020-04883-1.
[7] K. Ravindran, T.W. Rogers, T. Yuen, F. Gaillard, Intracranial white epidermoid cyst with dystrophic calcification - a case report and literature review, J. Clin. Neurosci. 42 (2017) 43–47, https://doi.org/10.1016/j.jocn.2017.03.006.
[8] C. Daugherty, T. Ngo, D. Drehner, T. Maugans, Mature teratoma confined to the posterior fossa, Pediatr. Neurosurg. 51 (2) (2016) 93–98, https://doi.org/10.1159/000442178.
[9] J.Y. Brown, A.P. Morokoff, P.J. Mitchell, M.F. Gonzales, Unusual imaging appearance of an intracranial dermoid cyst, AJNR Am J Neuroradiol 22 (10) (2001) 1970–1972.
[10] S.P. Kumaran, R. Srinivasa, N. Ghosal, Unusual radiological presentation of intracranial dermoid cyst: a case series, Asian J Neurosurg 14 (1) (2019) 269–271, https://doi.org/10.4103/ajns.AJNS_304_17.
[11] X. Wang, Y. Yu, X. Zhang, F. Hu, Y. Gu, T. Xie, H. Yu, Z. Cai, Unusual imaging appearance of a huge intracranial dermoid cyst located across the anterior and middle skull base, J. Neurol. Surg. Cent. Eur. Neurosurg. 74 (Suppl 1) (2013) e185–e187, https://doi.org/10.1055/s-0033-1337610.
[12] X. Wang, Y. Yu, X. Zhang, F. Hu, Y. Gu, T. Xie, H. Yu, Z. Cai, Unusual imaging appearance of a huge intracranial dermoid cyst located across the anterior and middle skull base, J. Neurol. Surg. Cent. Eur. Neurosurg. 74 (Suppl 1) (2013) e185–e187, https://doi.org/10.1055/s-0033-1337610.
[13] M. Bohara, H. Yonezawa, P. Karki, Y. Bakhtiar, H. Hirano, I. Kitazono, N. Matsuyama, K. Arita, Mature posterior fossa teratoma mimicking dermoid cyst, Brain Tumor Pathol. 30 (4) (2013) 262–265, https://doi.org/10.1007/s10014-012-0129-6.
[14] P.F. New, S. Aronow, Attenuation measurements of whole blood and blood fractions in computed tomography, Radiology 121 (3 Pt. 1) (1976) 635–640, https://doi.org/10.1148/121.3.635.

[15] R.L. Baron, C.A. Rohrmann Jr., S.P. Lee, W.P. Shuman, S.A. Teefey, CT evaluation of gallstones in vitro: correlation with chemical analysis, AJR Am. J. Roentgenol. 151 (6) (1988) 1123–1128, https://doi.org/10.2214/ajr.151.6.1123.
[16] M.H. Lipper, P.R. Kishore, J.D. Ward, Craniopharyngioma: unusual computed tomographic presentation, Neurosurgery 9 (1) (1981) 76–78, https://doi.org/10.1227/00006123-198107000-00014.
[17] F.A. Timmer, M. Sluzewski, M. Treskes, W.J. van Rooij, J.L. Teepen, D. Wijnalda, Chemical analysis of an epidermoid cyst with unusual CT and MR characteristics, AJNR Am J Neuroradiol 19 (6) (1998) 1111–1112.
[18] I.F. Braun, R.S. Pinto, F. Epstein, Dense cystic craniopharyngiomas, AJNR Am J Neuroradiol 3 (2) (1982) 139–141.
[19] P.M. Som, W.P. Dillon, G.D. Fullerton, R.A. Zimmerman, B. Rajagopalan, Z. Marom, Chronically obstructed sinonasal secretions: observations on T1 and T2 shortening, Radiology 172 (2) (1989) 515–520, https://doi.org/10.1148/radiology.172.2.2748834.
[20] M. Takeshita, O. Kubo, H. Hiyama, Y. Tajika, M. Izawa, M. Kagawa, K. Takakura, N. Kobayashi, M. Toyoda, Magnetic resonance imaging and quantitative analysis of contents of epidermoid and dermoid cysts, Neurol. Med.-Chir. 34 (7) (1994) 436–439, https://doi.org/10.2176/nmc.34.436.
[21] H. Nakata, Y. Sato, T. Nakayama, H. Yoshimatsu, T. Kobayashi, Bronchogenic cyst with high CT number: analysis of contents, J. Comput. Assist. Tomogr. 10 (2) (1986) 360, https://doi.org/10.1097/00004728-198603000-00044.
[22] M. Ochi, K. Hayashi, T. Hayashi, M. Morikawa, A. Ogino, R. Hashmi, M. Iwanaga, A. Yasunaga, S. Shibata, Unusual CT and MR appearance of an epidermoid tumor of the cerebellopontine angle, AJNR Am J Neuroradiol 19 (6) (1998) 1113–1115.
[23] S. Kuwabara, H. Seo, S. Ishikawa, Huge, dense, cystic craniopharyngioma with unusual extensions–case report, Neurol. Med.-Chir. 27 (1) (1987) 37–41, https://doi.org/10.2176/nmc.27.37.
[24] J. Ahmadi, F. Savabi, M.L. Apuzzo, H.D. Segall, D. Hinton, Magnetic resonance imaging and quantitative analysis of intracranial cystic lesions: surgical implication, Neurosurgery 35 (2) (1994) 199–207, https://doi.org/10.1227/00006123-199408000-00004, discussion 207.
[25] S. Nagasawa, H. Handa, J. Yamashita, Y. Kinuta, Dense cystic craniopharyngioma with unusual extensions, Surg. Neurol. 19 (3) (1983) 299–301, https://doi.org/10.1016/s0090-3019(83)80021-4.
[26] J. Ahmadi, S. Destian, M.L. Apuzzo, H.D. Segall, C.S. Zee, Cystic fluid in craniopharyngiomas: MR imaging and quantitative analysis, Radiology 182 (3) (1992) 783–785, https://doi.org/10.1148/radiology.182.3.1535894.
[27] D.B. Hackney, R.I. Grossman, R.A. Zimmerman, P.M. Joseph, H.I. Goldberg, L.T. Bilaniuk, M.V. Spagnoli, Low sensitivity of clinical MR imaging to small changes in the concentration of nonparamagnetic protein, AJNR Am J Neuroradiol 8 (6) (1987) 1003–1008.
[28] R.K. Gupta, R. Pandey, E.M. Khan, P. Mittal, R.B. Gujral, D.K. Chhabra, Intracranial tuberculomas: MRI signal intensity correlation with histopathology and localised proton spectroscopy, Magn. Reson. Imaging 11 (3) (1993) 443–449, https://doi.org/10.1016/0730-725x(93)90079-s.
[29] I. Isiklar, N.E. Leeds, G.N. Fuller, A.J. Kumar, Intracranial metastatic melanoma: correlation between MR imaging characteristics and melanin content, AJR Am. J. Roentgenol. 165 (6) (1995) 1503–1512, https://doi.org/10.2214/ajr.165.6.7484597.
[30] S.S. Kim, M.H. Han, J.E. Kim, C.H. Lee, H.W. Chung, J.S. Lee, K.H. Chang, Malignant melanoma of the sinonasal cavity: explanation of magnetic resonance signal intensities with histopathologic characteristics, Am. J. Otolaryngol. 21 (6) (2000) 366–378, https://doi.org/10.1053/ajot.2000.18865.
[31] J.J. Greenberg, R.F. Oot, G.L. Wismer, K.R. Davis, M.L. Goodman, A.E. Weber, W.W. Montgomery, Cholesterol granuloma of the petrous apex: MR and CT evaluation, AJNR Am J Neuroradiol 9 (6) (1988) 1205–1214.
[32] B.O. Kjos, M. Brant-Zawadzki, W. Kucharczyk, W.M. Kelly, D. Norman, T.H. Newton, Cystic intracranial lesions: magnetic resonance imaging, Radiology 155 (2) (1985) 363–369, https://doi.org/10.1148/radiology.155.2.3983386.
[33] P. Vock, L.W. Hedlund, R.J. Herfkens, E.L. Effmann, M.A. Brown, C.E. Putman, Work in progress: in vitro analysis of pleural fluid analogs by proton magnetic resonance. Preliminary studies at 1.5T, Invest. Radiol. 22 (5) (1987) 382–387, https://doi.org/10.1097/00004424-198705000-00005.
[34] M. Epelman, A. Daneman, S.I. Blaser, C. Ortiz-Neira, O. Konen, J. Jarrín, O.M. Navarro, Differential diagnosis of intracranial cystic lesions at head US: correlation with CT and MR imaging, Radiographics 26 (1) (2006) 173–196, https://doi.org/10.1148/rg.261055033.
[35] C.H. Hsieh, K.M. Huang, M.C. Kao, et al., Hemorrhage in intracranial epidermoid cyst, J. Formos. Med. Assoc. 95 (1996) 173–175.
[36] Y. Inoue, K. Ohata, K. Nakayama, T. Haba, M. Shakudo, An unusual middle fossa interdural epidermoid tumor. Case report, J. Neurosurg. 95 (5) (2001) 902–904, https://doi.org/10.3171/jns.2001.95.5.0902.
[37] H. Tsurushima, T. Kamezaki, Y. Tomono, T. Nose, Intracranial epidermoid cyst including elements of old hematoma, Neurol. Med.-Chir. 37 (11) (1997) 861–864, https://doi.org/10.2176/nmc.37.861.
[38] S.C. Niesporek, S.H. Hoffmann, M.C. Berger, N. Benkhedah, A. Kujawa, P. Bachert, A.M. Nagel, Partial volume correction for in vivo (23)Na-MRI data of the human brain, Neuroimage 112 (2015) 353–363, https://doi.org/10.1016/j.neuroimage.2015.03.025.
[39] S.H. Koenig, R.D. Brown 3rd, T.R. Lindstrom, Interactions of solvent with the heme region of methemoglobin and fluoro-methemoglobin, Biophys. J. 34 (3) (1981) 397–408, https://doi.org/10.1016/S0006-3495(81)84858-8.
[40] J.L. Barnhart, R.N. Berk, Influence of paramagnetic ions and pH on proton NMR relaxation of biologic fluids, Invest. Radiol. 21 (2) (1986) 132–136, https://doi.org/10.1097/00004424-198602000-00009.
[41] M.Z. Köylü, S. Asubay, A. Yilmaz, Determination of proton relaxivities of Mn(II), Cu(II) and Cr(III) added to solutions of serum proteins, Molecules 14 (4) (2009) 1537–1545, https://doi.org/10.3390/molecules14041537.
[42] N. Zhang, V.A. Fitsanakis, K.M. Erikson, M. Aschner, M.J. Avison, J.C. Gore, A model for the analysis of competitive relaxation effects of manganese and iron in vivo, NMR Biomed. 22 (4) (2009) 391–404, https://doi.org/10.1002/nbm.1348.
[43] D.R. Warakaulle, P. Anslow, Differential diagnosis of intracranial lesions with high signal on T1 or low signal on T2-weighted MRI, Clin. Radiol. 58 (12) (2003) 922–933, https://doi.org/10.1016/s0009-9260(03)00268-x.